Applied and Environmental Microbiology, July 2008, p. 4440–4453 Vol. 74, No. 14
0099-2240/08/$08.00+0 doi:10.1128/AEM.02692-07

Characterization of Nitrifying, Denitrifying, and Overall Bacterial Communities in Permeable Marine Sediments of the Northeastern Gulf of Mexico▽†

Heath J. Mills,[1,2] Evan Hunter,[1] Mike Humphrys,[1] Lee Kerkhof,[3] Lora McGuinness,[3] Markus Huettel,[1] and Joel E. Kostka[1]*

Department of Oceanography, Florida State University, Tallahassee, Florida 32306[1]; Department of Oceanography, Texas A&M University, College Station, Texas 77843[2]; and Institute of Marine and Coastal Sciences, Rutgers University, New Brunswick, New Jersey 08901[3]

Received 29 November 2007/Accepted 12 May 2008

Sandy or permeable sediment deposits cover the majority of the shallow ocean seafloor, and yet the associated bacterial communities remain poorly described. The objective of this study was to expand the characterization of bacterial community diversity in permeable sediment impacted by advective pore water exchange and to assess effects of spatial, temporal, hydrodynamic, and geochemical gradients. Terminal restriction fragment length polymorphism (TRFLP) was used to analyze nearly 100 sediment samples collected from two northeastern Gulf of Mexico subtidal sites that primarily differed in their hydrodynamic conditions. Communities were described across multiple taxonomic levels using universal bacterial small subunit (SSU) rRNA targets (RNA- and DNA-based) and functional markers for nitrification (*amoA*) and denitrification (*nosZ*). Clonal analysis of SSU rRNA targets identified several taxa not previously detected in sandy sediments (i.e., *Acidobacteria*, *Actinobacteria*, *Chloroflexi*, *Cyanobacteria*, and *Firmicutes*). Sequence diversity was high among the overall bacterial and denitrifying communities, with members of the *Alphaproteobacteria* predominant in both. Diversity of bacterial nitrifiers (*amoA*) remained comparatively low and did not covary with the other gene targets. TRFLP fingerprinting revealed changes in sequence diversity from the family to species level across sediment depth and study site. The high diversity of facultative denitrifiers was consistent with the high permeability, deeper oxygen penetration, and high rates of aerobic respiration determined in these sediments. The high relative abundance of *Gammaproteobacteria* in RNA clone libraries suggests that this group may be poised to respond to short-term periodic pulses of growth substrates, and this observation warrants further investigation.

Permeable marine sediments, and their associated bacterial communities, act as biocatalytic filters for the overlying water column in the coastal ocean. Nearly half of the biomass produced from primary production is thought to deposit onto the shallow continental shelf seafloor, where highly active bacterial communities mineralize the organic matter and release inorganic nutrients back into the water column (11, 32, 34, 38, 63). Thus, enhanced pore water exchange in permeable sediments or sands may stimulate bacterial metabolism through the delivery of substrates and the removal of metabolites (7, 11, 35). Due to the high permeability of these sediments, hydrodynamic forces likely affect the bacterial niches within the uppermost layer of the seabed and impact overall bacterial diversity (33). Although more information is available on bacterial communities present in less permeable, muddy sediments (37), relatively few studies have investigated the microbiology of marine sands, and thus little is known about the diversity of microorganisms inhabiting these environments.

Nitrogen often limits primary production in marine environments (30), and the predominant sink or loss of nitrogen in the coastal ocean is nitrification-denitrification. Nitrification and denitrification are bacterially mediated processes that, when coupled, link the mineralization of nitrogenous compounds to the liberation of gaseous nitrogen that can be released to the atmosphere (15, 42, 70). Understanding the diversity of the bacterial groups associated with nitrification and denitrification is critical to understanding the factors that may influence this important part of the nitrogen cycle in the marine environment. In order to elucidate the nitrifier communities, the functional gene, *amoA*, was assayed which encodes the first subunit of ammonia monooxygenase, a protein involved in the first step of nitrification. This gene has been used to identify nitrifiers, and a previous study by Hunter et al. (33) reported a low diversity of *amoA* genes in sandy marine sediments. However, a limited number of samples were examined, and very little is known about the diversity of bacterial *amoA* genes in permeable marine sediments across environmental gradients. For monitoring denitrifying bacteria in marine environments, three functional genes (*nirS*, *nirK*, and *nosZ*) have been used to (9, 10, 43, 66, 67) due to their broad phylogenetic diversity. While *nirS* and *nirK* encode enzymes active early in the denitrification pathway, *nosZ* encodes the enzyme nitrous oxide reductase, which catalyzes the final step in denitrification, thus representing the process that leads to the loss of biologically available nitrogen from the sediment. Although reports of

* Corresponding author. Mailing address: Department of Oceanography, Florida State University, FSU Collins Research Lab, 255 Atomic Way, Bldg. 42, Tallahassee, FL 32306-4470. Phone: (850) 644-5719. Fax: (850) 644-2581. E-mail: jkostka@ocean.fsu.edu.

† Supplemental material for this article may be found at http://aem.asm.org/.

▽ Published ahead of print on 16 May 2008.

TABLE 1. Biogeochemical characteristics of gulf and bay sediments sampled in March and May

Parameter[a]	Gulf[b]		Bay[c]	
	March	May	March	May
Median grain size (μm)*	180.9	209.6	307.0	220.0
Sorting coefficient*	1.5	1.8	1.6	1.6
Porosity (%)†	40.3 ± 0.4	40.1 ± 0.6	39.8 ± 1.3	42.6 ± 0.5
Mean permeability (m^2) ± SD†	$(2.0 \times 10^{-11}) \pm (1.7 \times 10^{-12})$	$(2.8 \times 10^{-11}) \pm (8.2 \times 10^{-13})$	$(4.6 \times 10^{-11}) \pm (1.2 \times 10^{-11})$	$(3.4 \times 10^{-11}) \pm (6.9 \times 10^{-12})$
Oxygen production (mmol m^{-2} day^{-1})†	14.17	51.36	81.85	34.70
Oxygen consumption (mmol m^{-2} day^{-1})§	–11.82	–19.54	–17.11	–16.56
Photosynthesis (mmol m^{-2} day^{-1})§	25.98	70.90	98.96	51.26
Mean C content (%) ± SD**	0.12 ± 0.1	0.11	0.11 ± 0.1	0.14

[a] *, Calculated according to the method of Blott and Pye (6); †, calculated according to the method of Holme and McIntyre (28); †, calculated according to the method of Cook et al. (18); §, calculated from oxygen production corrected for sediment oxygen consumption during daylight; **, calculated in a CarloErba Element CNS analyzer, with sulfanilamide as a standard.
[b] Slightly gravelly fine sand, moderately sorted.
[c] Slightly gravelly fine sand, moderately well sorted.

denitrifier diversity in continental shelf sediments have been published (66–68), the database for marine sediments remains small, and past studies have often focused on methodological development.

The objective of the present study was to expand the characterization of bacterial community diversity in understudied permeable shelf sediments across spatial, temporal, and hydrodynamic gradients. Simultaneous purification and analysis of community DNA and RNA compared total and metabolically active bacterial populations. High-throughput techniques were developed and coupled with clonal analysis to facilitate the determination of overall, denitrifier, and nitrifier bacterial community composition at increased spatial resolution. Whereas clonal analysis revealed no substantial changes across environmental gradients, terminal restriction fragment length polymorphism (TRFLP) profiles showed distinct differences in bacterial community composition according to site, depth, and time period sampled.

MATERIALS AND METHODS

Site and sample description. Permeable marine sediments were studied on St. George Island, FL, in the northeastern Gulf of Mexico (NEGOM). The continental shelf near St. George Island is considered to be relatively pristine and unaffected by heavy anthropogenic impact. Sediment samples were collected in March and May 2005 from the gulf (29°44.885N, 84°42.594W) and from Apalachicola Bay (29°45.034N, 84°42.719W) sides of St. George Island and were comprised predominantly of moderately well-sorted quartz sand with a relatively low organic matter content (<0.2%) and a porosity of 40 to 43% (Table 1). More information on these biogeochemical determinations can be found in the Table 1. Water depths at the study site ranged from 1 to 2 m, and bottom currents (<0.6 m s^{-1}) were dominated by tidal and wave-induced currents. The sediment surface on the gulf side had sand ripples 2 to 3 cm in height, and these were spaced 7 to 10 cm apart, while the bay side contained sand ripples 0.5 to 1 cm in height, spaced 3 to 5 cm apart, reflecting a stronger wave impact on the gulf side. Divers manually collected triplicate cores at each site by using polycarbonate core liners (3.6-cm inner diameter; 20 to 25 cm in height). All cores were immediately frozen on dry ice and stored at −80°C. Each core was cryosectioned into seven different depth intervals: 0 to 2 cm, 2 to 4 cm, 4 to 6 cm, 6 to 8 cm, 8 to 10 cm, 14 to 16 cm, and 18 to 20 cm.

Nucleic acid extraction and analysis of small-subunit (SSU) rRNA, *nosZ*, and *amoA* gene targets. Community DNA was extracted from sediment samples by using a phenol-chloroform procedure adapted from that of Kerkhof and Ward (41). The main deviation from the original method included the use of liquid nitrogen and a 55°C water bath for the freeze-thaw steps. A portion of the nucleic acid extract was then cleaned by using the Wizard DNA Clean-Up system (Promega, Madison, WI). Individual extracts from each depth from triplicate cores were combined prior to PCR amplification, resulting in an array of 28 DNA extracts (i.e., seven depths × two sites × two sample dates) used to profile the bacterial community. Portions of the nucleic acid extractions were also RNA purified by using an RNA/DNA Midi kit (Qiagen, Valencia, CA) according to the manufacturer's instructions. Residual DNA was removed from RNA extracts with 5 U of RQ1 RNase-free DNase (Promega) according to the manufacturer's instructions.

Bacterial SSU rRNA, *nosZ*, and *amoA* genes were amplified by PCR. General reaction conditions included a standard PCR mix (1× PCR buffer containing 1.5 mM $MgCl_2$ [Takara Bio, Inc., Japan], 250 μM concentrations of each deoxynucleoside triphosphate [Takara Bio], 1 to 15 pmol each of forward and reverse primers, 1 to 2 U of *Taq* polymerase [Takara Bio], deionized H_2O, and 10 to 20 ng of DNA). The primer sequences and specific PCR conditions for DNA amplification are listed in Table 2.

Aliquots of rRNA were reverse transcribed to cDNA using Moloney murine leukemia virus reverse transcriptase and *Bacteria* domain-specific SSU rRNA reverse primer 518R (59) according to the manufacturer's instructions (Promega). Then, 10 to 50 ng of cDNA was used in a standard PCR with *Bacteria* domain-specific 27F (39) and 518R (59) primers. The PCR amplification conditions are listed in Table 2. DNA contamination of RNA extracts was routinely monitored by PCR amplification of RNA extracts that had not been reverse transcribed. No contaminating DNA was detected in any of these reactions. Amplicons from both DNA- and RNA-based reactions were visualized by gel electrophoresis on a 0.7% agarose gels, stained with ethidium bromide, and UV illuminated.

PCR and reverse transcription-PCR products were cleaned by using a Qiagen PCR purification kit and cloned by using a TOPO TA cloning kit (Invitrogen, Carlsbad, CA) according to the manufacturer's instructions. A total of 15 libraries (4 SSU rRNA gene [DNA derived], 4 SSU rRNA [RNA derived], 4 *nosZ*, and 3 *amoA*) were constructed from bay and gulf sediment samples collected from the 0- to 2-cm and 18- to 20-cm depth intervals. No *amoA* amplification was detected in DNA extracted from either of the three individual or combined March bay cores at 18- to 20-cm depth; thus, three *amoA* clone libraries were constructed. Cloned inserts were amplified by using the vector-specific primers M13F and M13R (50) and corresponding PCR conditions (Table 2). After amplicon size verification, 1 μg of the clone PCR product was digested by using HaeIII (New England Biolabs, Inc., Beverly, MA) and MspI (Promega) restriction enzymes for 2.5 h at 37°C according to the manufacturer's instructions for RFLP analysis. Digested DNA fragments were size fractionated by a 2% agarose gel stained with ethidium bromide and visualized by using a Bio-Rad GelDoc XR system (Bio-Rad Laboratories, Inc., Hercules, CA). DNA fragment sizes were estimated by comparison to molecular mass standards (1-kb and 50-bp DNA ladder; Promega). Clones were grouped into phylotypes according to banding patterns with representatives of select SSU rRNA and SSU rRNA gene phylotypes (i.e., phylotypes containing more than one clone), and all *nosZ* and *amoA* gene phylotypes were bidirectionally sequenced by using an Applied Biosystems 3100 genetic analyzer (ABI, Foster City, CA) at the Florida State University sequencing facility. Select phylotypes with banding patterns that matched previously sequenced phylotypes from Hunter et al. (33) were sequenced to verify similarity between studies. Clones with designations beginning LC or SC are from Hunter et al. (33) and represent phylotypes detected in both studies.

TABLE 2. Oligonucleotide primer pairs and PCR conditions used in this study

Primer	Specificity	Annealing temp (°C)	Product size (bp)	Sequence (5′–3′)	Source or reference
27F	Domain *Bacteria*	55	1,365	AGR GTT TGA TCM TGG CTC AG	23a
1392R				ACG GGC GGT GTG TRC	41a
518R	Domain *Bacteria*	50	491[a]	CGT ATT ACC GCG GCT GCT GG	59
nos752	*nosZ*	55	1,021	ACC GAY GGS ACC TAY GAY GG	L. McGuinness and L. J. Kerkhof, unpublished data
nos1773R				ATR TCG ATC ARC TGB TCG TT	L. McGuinness and L. J. Kerkhof, unpublished data
amoA-1F	*amoA*	60		GGG GTT TCT ACT GGT GGT	64a
amoA-2R				CCC CTC KGS AAA GCC TTC TTC	64a
M13F	pCR2.1 vector	55	Variable	GTA AAA CGA CGG CCA G	50
M13R				CAG GAA ACA GCT ATG AC	50

[a] Product size based on the forward primer being 27F.

TRFLP analysis. For TRFLP, the bacterial SSU rRNA and *nosZ* genes were PCR amplified from the same community DNA used for clone library construction. Similar PCR amplification conditions were used as described above, except the forward primers were labeled with 6-carboxyfluorescien (ABI). Fluorescent amplification of *amoA* was unsuccessful due to gene template concentrations being below our detection limit. TRFLP analysis of SSU rRNA and *nosZ* genes was performed according to the method of Kerkhof et al. (40) using MnlI as the restriction enzyme and the forward primers listed in Table 2. TRFLP fingerprinting was performed on an ABI 310 genetic analyzer (ABI) using Genescan software. To identify individual peaks, the 5′ terminal restriction fragment (TRF) length for each sequenced clone was determined by an in silico digest using the MnlI recognition site and matched to the peak sizes from the TRFLP analysis. Ten phylotypes were chosen at random to have in silico digests verified by individual TRFLP analysis. For each phylotype, the in silico predictions were within one base of the size observed on TRFLP electropherograms with a majority being exact matches. In silico digests from Hunter et al. (33) were also included in the analysis of TRFLP profiles. Similar TRF lengths that were obtained from multiple unrelated clone sequences were discarded, and associated electropherogram peaks were not included in statistical calculations. TRFs from representative phylotype sequences were matched to peaks from each of the 28 sediment sample profiles (i.e., seven depths, two sites, and two months). Further, comparative analysis of the TRFLP profiles was performed based on the Sorenson's similarity index (47, 56) and UPGMA (for unweighted pair-group method with arithmetic averages) analysis using the COMbinatorial Polythetic Agglomerative Hierarchical clustering package (COMPAH96; http://www.es.umb.edu/edgwebp.htm). Dendrograms were constructed by inserting distance matrices into Clustering Calculator (www2.biology.ualberta.ca/jbrzusto/cluster.php#ClusterCalc) using Canberra Distance for distance measure and Saitou and Nei neighbor-joining for the clustering method. Output trees were visualized on TreeView (taxonomy.zoology.gla.ac.uk/rod/treeview.html).

Phylogenetic and statistical analyses. All clone sequences were checked for chimeras using Chimera Check from the Ribosomal Database Project II Release 9 (48). Sequences from the present study and reference sequences, as determined by highest sequence similarity during BLAST analysis, were subsequently aligned by using the Fast Aligner algorithm in the ARB package (71). All SSU rRNA alignments were visually verified and manually adjusted according to *Escherichia coli* SSU rRNA secondary structure. According to the method of Hunter et al. (33), neighbor-joining trees incorporating a Jukes-Cantor distance correction were created from the alignments using the ARB software package (71). An average of 500 (i.e., *amoA*) to 1,000 (i.e., SSU rRNA and *nosZ* clones) nucleotides were included in the phylogenetic analyses. Bootstrap data represented 1,000 samplings. RNA derived SSU rRNA clones were not included in tree construction due to the reduced lengths of cloned sequences (~500 bp) available for comparison. Rarefaction analysis was performed using equations described by Heck et al. (27). The percent coverage (C) of the clone libraries was calculated according to the following equation: $C = [1 - (n_i/N)] \times 100$ (24, 54), where n_i is the number of unique clones as determined by RFLP analysis, and N is the total number of clones in the library. Sorensen's index, the Shannon-Wiener index, and species richness were determined by EstimateS (14, 16, 17).

Nucleotide sequence accession numbers. The 52 total nucleotide SSU rRNA, *nosZ*, and *amoA* sequences reported here were submitted to the GenBank database under accession numbers DQ431855 to DQ431906.

RESULTS

Sediment characteristics and biogeochemical rate measurements. Bulk-phase sediment characteristics and organic matter content between the gulf and bay sites or the different sampling times were largely the same (Table 1). The observed production and consumption rates of oxygen are among the highest rates measured for shallow subtidal marine sediments and indicate that the turnover of organic matter in the marine sands of the NEGOM equals or exceeds that of muddy sediments in similar subtidal locations. Oxygen consumption rates, a proxy for organic matter degradation, were similar between the sites and times (Table 1). Photosynthetic production was about four times higher at the bay site in comparison to the gulf site during March, but lower in May. A distinct difference in the heights and spacing of sand ripples was observed that can be attributed to the fact that the gulf site is exposed to stronger waves and currents in comparison to the bay site. When the bottom currents generated by waves and tides are deflected by the ripple topography, pressure gradients develop that pump water through the upper layers of the permeable sediments. In situ tracer clearing rate measurements with benthic advection chambers (11, 32, 34, 38, 63) revealed that under moderate bottom currents of 10 cm s^{-1} approximately 461 ± 94 (standard deviation [SD]) liters m^{-2} day^{-1} are filtered through the upper 6 cm of the gulf sediment. In contrast on the bay side, filtration reached only 137 ± 13 (SD) liters m^{-2} day^{-1} with a pore water penetration of 3 cm. During stormy periods, these filtration rates and filtration depth could be doubled. The contrasting hydrodynamic conditions and ensuing flushing depths at the two study sites were also reflected in the stratification of iron minerals present in sediment cores, observed as a color change from brown Fe(III) oxides to black Fe(II) sulfides. A distinct redox transition was observed in bay site cores at a depth of approximately 4 cm, whereas no such stratification was observed in gulf site cores.

TABLE 3. Statistical analyses of SSU rRNA and *nosZ* gene clone libraries using standard ecological and molecular estimates of sequence diversity

PCR target	Sample	No. of clones (no. of phylotypes)	% Coverage	Species richness (95% CI)[a]	Shannon-Weiner index	1/D
SSU rRNA gene (DNA)	3B02	70 (38)	42	64 (48–101)	3.44	40.3
	3B1820	67 (44)	36	85 (63–132)	3.66	67.0
	3G02	55 (34)	32	66 (47–110)	3.34	38.1
	3G1820	57 (31)	42	50 (38–83)	3.25	34.0
	Total	249 (71)	66	92 (80–122)	3.89	42.2
SSU rRNA (RNA)	3B02	26 (18)	54	29 (21–55)	2.81	37.5
	3B1820	39 (20)	69	37 (25–74)	2.78	19.5
	3G02	39 (26)	54	52 (36–94)	3.11	35.3
	3G1820	32 (15)	87	16 (15–22)	2.62	21.1
	Total	136 (42)	88	57 (47–85)	3.41	28.5
nosZ	3B02N	27 (13)	54	18 (14–39)	2.42	15.3
	3B1820N	33 (18)	39	38 (23–105)	2.68	17.6
	3G02N	81 (27)	52	41 (31–78)	2.67	8.2
	3G1820N	90 (23)	65	28 (24–48)	2.70	12.3
	Total	231 (38)	74	46 (40–66)	3.03	14.1

[a] CI, confidence interval.

RFLP and statistical analyses of SSU rRNA, *nosZ*, and *amoA* clone libraries. Fifteen clone libraries constructed by using nucleic acids extracted from March bay 0- to 2-cm (3B02) and 18- to 20-cm (3B1820) and gulf 0- to 2-cm (3G02) and 18- to 20-cm (3G1820) sediment core sections resulted in a total of 249 *Bacteria* SSU rRNA gene clones (DNA-derived), 136 *Bacteria* SSU rRNA clones (RNA-derived), 231 *nosZ* clones, and 64 *amoA* clones. The sample abbreviations given in parentheses will henceforth be used to identify the clone sequences retrieved. Clone sequences with designations beginning with LC or SC are from Hunter et al. (33) and represent phylotypes detected in both studies. The percent coverage for all four SSU rRNA gene clone libraries was 66% (Table 3), with individual library coverage ranging from 32 to 42%. RNA-derived SSU rRNA clone libraries had higher percent coverages for the individual libraries (54 to 87%) and the combined, total library (88%). All diversity indices suggested lower diversity in the RNA-derived libraries compared to the corresponding DNA-derived libraries (Table 3). The total *nosZ* clone library, integrating all samples, had a calculated total percent coverage of 74% with lower individual clone library percent coverages (39 to 65%) (Table 3). Statistical estimators suggested the *nosZ* gene diversity was similar to that of the SSU rRNA (Table 3), but much higher than that of the *amoA* gene. Two phylotypes were detected in the three *amoA* clone libraries (see Table S1 in the supplemental material) with a percent coverage of 100% for each (data not shown). Rarefaction curves for the total SSU rRNA (DNA- and RNA-derived) and *nosZ* libraries and the total and individual *amoA* gene libraries suggested a sufficient number of clones were sampled to represent library diversity (see Fig. S1 in the supplemental material). Although rarefaction curves for the remaining libraries did not indicate sample saturation, sufficient clones were screened to indicate trends within the bacterial communities.

SSU rRNA gene phylogenetic analysis. Sequence analysis of 46 of the 73 SSU rRNA gene phylotypes (DNA-derived) indicated nine distinct phyla with a majority of the sequences most closely related to sequences of uncultured organisms obtained from other marine environments (see Table S2 in the supplemental material). Two separate distance-based neighbor-joining trees were constructed with 20 *Proteobacteria* and 26 non-*Proteobacteria*-related sequences from the present study, with additional reference sequences from the GenBank database providing classification of most sequences to the family taxonomic level (Fig. 1 and 2). Additional sequences indicated in boldface type the figures indicate clones with matching TRF lengths used in TRFLP analysis. Nearly half of the total SSU rRNA gene clones (46%) grouped within the phylum *Proteobacteria* (see Table S2 in the supplemental material). *Alphaproteobacteria*-related clones accounted for 56% of the total *Proteobacteria* (see Table S2 in the supplemental material). Similar to a previous sandy-sediment study (33), no clone sequences within the classes *Betaproteobacteria* and *Epsilonproteobacteria* were detected.

Proteobacteria. The 20 DNA-derived *Proteobacteria*-related phylotypes grouped into three classes, i.e., *Alpha-*, *Delta-*, and *Gammaproteobacteria*. A majority of the DNA-derived phylotypes ($n = 9$) was most closely related to the *Alphaproteobacteria* (see Table S2 in the supplemental material). Phylotypes 3G02-39 and LC1-35 clustered within the family *Hyphomicrobiaceae* (92 and 94%, respectively; Fig. 1) and were found in all four libraries, representing 31% of the *Alphaproteobacteria*-related clones (see Table S2 in the supplemental material). The six DNA-derived *Gammaproteobacteria*-related phylotypes (Fig. 1; SC1-11 and SC1-44 were only detected in TRFLP analysis and not in the clone libraries) exhibited little site or depth specificity. DNA-derived phylotypes 3G02-43 and 3B1820-38 represented 58% of the total *Deltaproteobacteria*-related clones and clustered within the group II sulfate reducer (46) family *Desulfobacteraceae* (see Table S2 in the supplemental material and Fig. 1), while phylotype SC3-7 clustered with the group III sulfate-reducing family *Desulfobulbaceae* (46) (Fig. 1). Representing 32% of the total *Deltaproteobacteria*-related clones, 3G02-06 and LC1-13 formed their own clade and could not be further classified beyond the class level (Fig. 1).

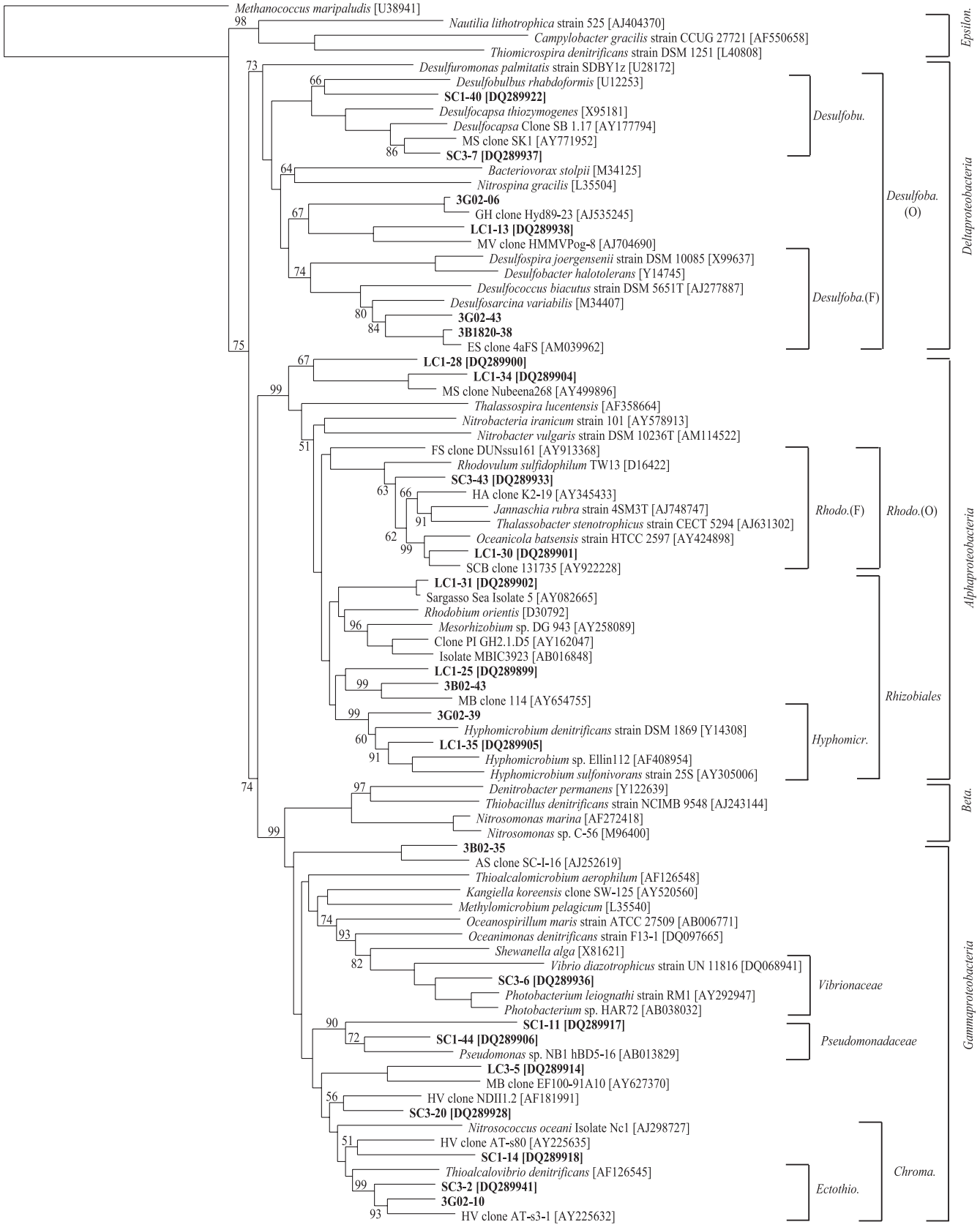
Methanococcus maripaludis [U38941]
Nautilia lithotrophica strain 525 [AJ404370]
Campylobacter gracilis strain CCUG 27721 [AF550658]
Thiomicrospira denitrificans strain DSM 1251 [L40808]
Desulfuromonas palmitatis strain SDBY1z [U28172]
Desulfobulbus rhabdoformis [U12253]
SC1-40 [DQ289922]
Desulfocapsa thiozymogenes [X95181]
Desulfocapsa Clone SB 1.17 [AY177794]
MS clone SK1 [AY771952]
SC3-7 [DQ289937]
Bacteriovorax stolpii [M34125]
Nitrospina gracilis [L35504]
3G02-06
GH clone Hyd89-23 [AJ535245]
LC1-13 [DQ289938]
MV clone HMMVPog-8 [AJ704690]
Desulfospira joergensenii strain DSM 10085 [X99637]
Desulfobacter halotolerans [Y14745]
Desulfococcus biacutus strain DSM 5651T [AJ277887]
Desulfosarcina variabilis [M34407]
3G02-43
3B1820-38
ES clone 4aFS [AM039962]
LC1-28 [DQ289900]
LC1-34 [DQ289904]
MS clone Nubeena268 [AY499896]
Thalassospira lucentensis [AF358664]
Nitrobacteria iranicum strain 101 [AY578913]
Nitrobacter vulgaris strain DSM 10236T [AM114522]
FS clone DUNssu161 [AY913368]
Rhodovulum sulfidophilum TW13 [D16422]
SC3-43 [DQ289933]
HA clone K2-19 [AY345433]
Jannaschia rubra strain 4SM3T [AJ748747]
Thalassobacter stenotrophicus strain CECT 5294 [AJ631302]
Oceanicola batsensis strain HTCC 2597 [AY424898]
LC1-30 [DQ289901]
SCB clone 131735 [AY922228]
LC1-31 [DQ289902]
Sargasso Sea Isolate 5 [AY082665]
Rhodobium orientis [D30792]
Mesorhizobium sp. DG 943 [AY258089]
Clone PI GH2.1.D5 [AY162047]
Isolate MBIC3923 [AB016848]
LC1-25 [DQ289899]
3B02-43
MB clone 114 [AY654755]
3G02-39
Hyphomicrobium denitrificans strain DSM 1869 [Y14308]
LC1-35 [DQ289905]
Hyphomicrobium sp. Ellin112 [AF408954]
Hyphomicrobium sulfonivorans strain 25S [AY305006]
Denitrobacter permanens [Y122639]
Thiobacillus denitrificans strain NCIMB 9548 [AJ243144]
Nitrosomonas marina [AF272418]
Nitrosomonas sp. C-56 [M96400]
3B02-35
AS clone SC-I-16 [AJ252619]
Thioalcalomicrobium aerophilum [AF126548]
Kangiella koreensis clone SW-125 [AY520560]
Methylomicrobium pelagicum [L35540]
Oceanospirillum maris strain ATCC 27509 [AB006771]
Oceanimonas denitrificans strain F13-1 [DQ097665]
Shewanella alga [X81621]
Vibrio diazotrophicus strain UN 11816 [DQ068941]
SC3-6 [DQ289936]
Photobacterium leiognathi strain RM1 [AY292947]
Photobacterium sp. HAR72 [AB038032]
SC1-11 [DQ289917]
SC1-44 [DQ289906]
Pseudomonas sp. NB1 hBD5-16 [AB013829]
LC3-5 [DQ289914]
MB clone EF100-91A10 [AY627370]
HV clone NDII1.2 [AF181991]
SC3-20 [DQ289928]
Nitrosococcus oceani Isolate Nc1 [AJ298727]
HV clone AT-s80 [AY225635]
SC1-14 [DQ289918]
Thioalcalovibrio denitrificans [AF126545]
SC3-2 [DQ289941]
3G02-10
HV clone AT-s3-1 [AY225632]
Desulfobu.
Desulfoba.(F)
Desulfoba.
(O)
Rhodo.(F)
Rhodo.(O)
Hyphomicr.
Rhizobiales
Vibrionaceae
Pseudomonadaceae
Ectothio.
Chroma.
Epsilon.
Deltaproteobacteria
Alphaproteobacteria
Beta.
Gammaproteobacteria
0.10

Non-*Proteobacteria* lineages. Eight non-*Proteobacteria* phyla were identified by phylogenetic analysis. Of the 26 non-*Proteobacteria*-related phylotypes, 5 grouped within the phylum *Planctomycetes*, which contains the *Pirellula*-associated anammox functional group (Fig. 2). Although two phylotypes branch within the *Pirellula* clade, the other three phylotypes, represented by clones 3B1820-36, LC1-9, and LC1-1, diverged to form a second clade that was supported by strong bootstrap values (Fig. 2). The *Bacteroidetes*/*Chlorobi* superphylum contained six diverse phylotypes, accounting for 14% of the total SSU rRNA gene clones (Table 4), and was related to the orders *Sphingobacteriales* and *Chlorobiales* and the families *Saprospiraceae*, *Flexibacteraceae*, and *Flavobacteriaceae*. All *Acidobacteria*- and *Actinobacteria*-related phylotypes had low sequence similarity to identified cultured isolates; thus, classification beyond the phyla level was not possible (Fig. 2). Five of the six phylotypes in the phylum *Actinobacteria*, clustered within their own clade and apart from any cultured isolates (Fig. 2), with only SC3-41 (33) being affiliated with the cultured genus "*Candidatus* Microthrix parvicella" (89%). A single phylotype, 3B1820-43, clustered within the phylum *Cyanobacteria* and was 99% similar to the chloroplast DNA sequence from *Alnus incana* (Fig. 2 and see Table S2 in the supplemental material). Three phylotypes—LC1-24, 3G02-01, and 3G1820-58—clustered within the family *Anaerolinaceae* in the phylum *Chloroflexi* (Fig. 2). Phylotypes 3G02-02 and 3B1820-01 clustered with the families *Paenibacillaceae* and *Turicibacteraceae*, respectively, within the phylum *Firmicutes* (see Table S2 in the supplemental material and Fig. 2). The final two phylotypes, 3G1820-03 and 3G1820-56, branched into the aerobic heterotrophic phylum *Gemmatimonadetes* (Fig. 2).

SSU rRNA (RNA-derived) phylogenetic analysis. Sequence analysis of 23 of the 42 SSU rRNA phylotypes (RNA-derived) indicated six distinct phyla. Although *Firmicutes*, *Bacteriodetes*/*Chlorobi*, and *Gemmatimonadetes* were detected in the DNA-derived SSU rRNA gene libraries, no RNA-derived clones grouped into these phyla. Similar to the DNA-derived clones, nearly half of the RNA-derived clone sequences (41%) grouped into 12 *Proteobacteria*-related phylotypes; however, *Gammaproteobacteria*-related clones represented 59% of the total *Proteobacteria* (see Table S3 in the supplemental material).

Twelve RNA-derived *Proteobacteria*-related phylotypes grouped into three classes: *Alpha*-, *Delta*-, and *Gammaproteobacteria*. A majority of the DNA-derived phylotypes ($n = 9$) was most related to the *Alphaproteobacteria* (see Table S2 in the supplemental material), while only one RNA-derived phylotype grouped in this lineage. Six of the twelve *Proteobacteria*-related RNA-derived phylotypes grouped within the class *Gammaproteobacteria*. Although no *Pseudomonadaceae*-related clones were detected in the DNA-derived libraries, they were the most frequently detected *Gammaproteobacteria* lineage in the RNA-derived library (see Table S3 in the supplemental material) and were widely identified in the TRFLP profiles. *Deltaproteobacteria*-related phylotypes were more depth specific in RNA-derived libraries compared to the DNA-derived libraries.

A total of 11 RNA-derived non-*Proteobacteria*-related phylotypes grouped into five different phyla, all represented in the DNA-derived libraries. *Actinobacteria*, *Planctomycete*, and *Acidobacteria*-related phylotypes, incorporating 13, 12, and 5% of the total RNA-derived clones, respectively, were detected in all depths at each site (see Table S3 in the supplemental material). All three phylotypes related to phototrophic *Cyanobacteria* (11% of the total RNA-derived clones) were detected in the 18- to 20-cm libraries.

Phylogenetic analysis of the *nosZ* gene. Sequence analysis of the 42 *nosZ* gene phylotypes indicated that all sequences were most closely related to sequences of uncultured organisms that putatively clustered with *Alphaproteobacteria*-related *nosZ* genes (Fig. 3) However, due to low sequence similarity to cultured strains and the presence of *nosZ* on mobile genetic elements (69), characterization of these genes as being *Alphaproteobacteria*-related is reported with caution. The most frequently detected phylotype (17% of the total *nosZ* clones), 3G02N-02, was 81% similar to the environmental clone CSS bacterium 696M, retrieved from permeable sediments off the coast of New Jersey (66) (see Table S4 in the supplemental material). Several deep branching clades were comprised solely of clones from the South Atlantic Bight and NEGOM (Fig. 3) (2, 66).

TRFLP-based analysis of the bacterial community structure. Initially, triplicate samples from each site, depth, and time were analyzed by using TRFLP, resulting in 84 profiles (see representative profiles in Fig. 4). Comparative analysis, as described below, showed little difference between individual profiles and a sample formed by combining the triplicate extracts prior to fluorescent amplification. Thus, 28 profiles from the combined extracts were subjected to cluster analysis using pairwise Sorensen's indices to construct dendrograms for the bacterial and the denitrifier communities with the SSU rRNA and *nosZ* gene targets (Fig. 5). In contrast to the clonal analysis, the SSU rRNA and *nosZ* gene TRFLP profiles from gulf and bay samples formed separate and distinct clusters with less than 50 and 38% sequence similarity, respectively. Furthermore, all SSU rRNA gene gulf profiles from March and May clustered in separate clades (<63% similarity) and with the exception of the May 4-6 cm and 6-8 cm bay samples, all bay samples from March and May also formed distinct clusters (<52% similarity; Fig. 5A). The *nosZ*-derived TRFLP profiles

FIG. 1. Phylum *Proteobacteria* neighbor-joining phylogenetic tree, incorporating a Jukes-Cantor distance correction, of SSU rRNA gene sequences from 3B02, 3B1820, 3G02, and 3G1820 samples. Sequences from the present study and close relatives were aligned by using the Fast Aligner algorithm, verified by hand, and compared to the *E. coli* SSU rRNA secondary structure using the ARB software package. Sequence names in boldface type represent both cloned sequences and sequences from Hunter et al. (33) used in TRFLP peak analysis. Bootstrap analyses were conducted on 1,000 samples, and percentages greater than 50% are indicated at the nodes. *Methanococcus maripaludis* was used as the outgroup. Scale bar, 0.10 change per nucleotide position. Abbreviations: *Desulfobu*, *Desulfobulbaceae*; *Desulfoba*.(F), *Desulfobacteraceae*; *Desulfoba*.(O), *Desulfobacterales*; *Rhodo*.(F), *Rhodobacteraceae*; *Rhodo*.(O), *Rhodobacterales*; *Hyphomicr*., *Hyphomicrobiaceae*; *Ectothio*, *Ectothiorhodospiraceae*; *Chroma*., *Chromatiales*.

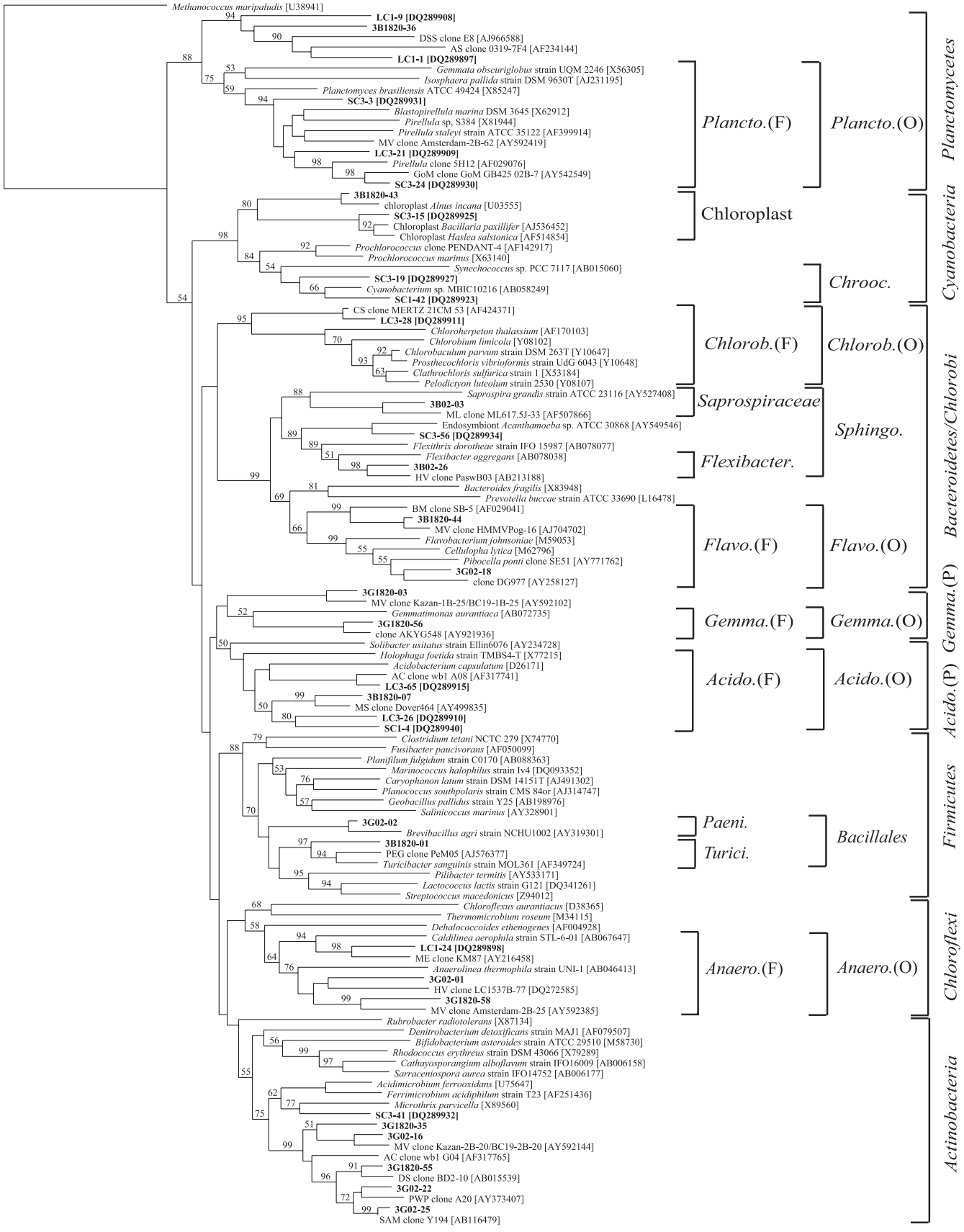
Methanococcus maripaludis [U38941]
LC1-9 [DQ289908]
3B1820-36
DSS clone E8 [AJ966588]
AS clone 0319-7F4 [AF234144]
LC1-1 [DQ289897]
Gemmata obscuriglobus strain UQM 2246 [X56305]
Isosphaera pallida strain DSM 9630T [AJ231195]
Planctomyces brasiliensis ATCC 49424 [X85247]
SC3-3 [DQ289931]
Blastopirellula marina DSM 3645 [X62912]
Pirellula sp, S384 [X81944]
Pirellula staleyi strain ATCC 35122 [AF399914]
MV clone Amsterdam-2B-62 [AY592419]
LC3-21 [DQ289909]
Pirellula clone 5H12 [AF029076]
GoM clone GoM GB425 02B-7 [AY542549]
SC3-24 [DQ289930]
3B1820-43
chloroplast Alnus incana [U03555]
SC3-15 [DQ289925]
Chloroplast Bacillaria paxillifer [AJ536452]
Chloroplast Haslea salstonica [AF514854]
Prochlorococcus clone PENDANT-4 [AF142917]
Prochlorococcus marinus [X63140]
Synechococcus sp. PCC 7117 [AB015060]
SC3-19 [DQ289927]
Cyanobacterium sp. MBIC10216 [AB058249]
SC1-42 [DQ289923]
CS clone MERTZ 21CM 53 [AF424371]
LC3-28 [DQ289911]
Chloroherpeton thalassium [AF170103]
Chlorobium limicola [Y08102]
Chlorobaculum parvum strain DSM 263T [Y10647]
Prosthecochloris vibrioformis strain UdG 6043 [Y10648]
Clathrochloris sulfurica strain 1 [X53184]
Pelodictyon luteolum strain 2530 [Y08107]
Saprospira grandis strain ATCC 23116 [AY527408]
3B02-03
ML clone ML617.5J-33 [AF507866]
Endosymbiont Acanthamoeba sp. ATCC 30868 [AY549546]
SC3-56 [DQ289934]
Flexithrix dorotheae strain IFO 15987 [AB078077]
Flexibacter aggregans [AB078038]
3B02-26
HV clone PaswB03 [AB213188]
Bacteroides fragilis [X83948]
Prevotella buccae strain ATCC 33690 [L16478]
BM clone SB-5 [AF029041]
3B1820-44
MV clone HMMVPog-16 [AJ704702]
Flavobacterium johnsoniae [M59053]
Cellulopha lytica [M62796]
Pibocella ponti clone SE51 [AY771762]
3G02-18
clone DG977 [AY258127]
3G1820-03
MV clone Kazan-1B-25/BC19-1B-25 [AY592102]
Gemmatimonas aurantiaca [AB072735]
3G1820-56
clone AKYG548 [AY921936]
Solibacter usitatus strain Ellin6076 [AY234728]
Holophaga foetida strain TMBS4-T [X77215]
Acidobacterium capsulatum [D26171]
AC clone wb1 A08 [AF317741]
LC3-65 [DQ289915]
3B1820-07
MS clone Dover464 [AY499835]
LC3-26 [DQ289910]
SC1-4 [DQ289940]
Clostridium tetani NCTC 279 [X74770]
Fusibacter paucivorans [AF050099]
Planifilum fulgidum strain C0170 [AB088363]
Marinococcus halophilus strain Iv4 [DQ093352]
Caryophanon latum strain DSM 14151T [AJ491302]
Planococcus southpolaris strain CMS 84or [AJ314747]
Geobacillus pallidus strain Y25 [AB198976]
Salinicoccus marinus [AY328901]
3G02-02
Brevibacillus agri strain NCHU1002 [AY319301]
3B1820-01
PEG clone PeM05 [AJ576377]
Turicibacter sanguinis strain MOL361 [AF349724]
Pilibacter termitis [AY533171]
Lactococcus lactis strain G121 [DQ341261]
Streptococcus macedonicus [Z94012]
Chloroflexus aurantiacus [D38365]
Thermomicrobium roseum [M34115]
Dehalococcoides ethenogenes [AF004928]
Caldilinea aerophila strain STL-6-01 [AB067647]
LC1-24 [DQ289898]
ME clone KM87 [AY216458]
Anaerolinea thermophila strain UNI-1 [AB046413]
3G02-01
HV clone LC1537B-77 [DQ272585]
3G1820-58
MV clone Amsterdam-2B-25 [AY592385]
Rubrobacter radiotolerans [X87134]
Denitrobacterium detoxificans strain MAJ1 [AF079507]
Bifidobacterium asteroides strain ATCC 29510 [M58730]
Rhodococcus erythreus strain DSM 43066 [X79289]
Cathayosporangium alboflavum strain IFO16009 [AB006158]
Sarraceniospora aurea strain IFO14752 [AB006177]
Acidimicrobium ferrooxidans [U75647]
Ferrimicrobium acidiphilum strain T23 [AF251436]
Microthrix parvicella [X89560]
SC3-41 [DQ289932]
3G1820-35
3G02-16
MV clone Kazan-2B-20/BC19-2B-20 [AY592144]
AC clone wb1 G04 [AF317765]
3G1820-55
DS clone BD2-10 [AB015539]
3G02-22
PWP clone A20 [AY373407]
3G02-25
SAM clone Y194 [AB116479]
Plancto.(F)
Chloroplast
Chrooc.
Chlorob.(F)
Saprospiraceae
Flexibacter.
Flavo.(F)
Gemma.(F)
Acido.(F)
Paeni.
Turici.
Anaero.(F)
Plancto.(O)
Chlorob.(O)
Sphingo.
Flavo.(O)
Gemma.(O)
Acido.(O)
Bacillales
Anaero.(O)
Planctomycetes
Cyanobacteria
Bacteroidetes/Chlorobi
Gemma.(P)
Acido.(P)
Firmicutes
Chloroflexi
Actinobacteria
0.10

from the bay March and May samples also showed a very distinct clustering (<52% similarity; Fig. 5B) with gulf March and May samples having less distinct clustering. These data are supported by the observation that 10 of the 23 TRFLP identified *nosZ* phylotypes were detected only in bay samples, while 6 were only found in gulf samples. Of note, for both gene targets, the 0- to 2-cm samples from the bay and gulf were more similar to the 18- to 20-cm samples from that same site compared to the other site's 0- to 2-cm sample.

In each of the 28 SSU rRNA TRFLP composite profiles, ca. 50% of the SSU rRNA gene-related peaks were identified and matched to clone phylotypes using in silico-derived TRF sizes. The *Alphaproteobacteria* identified TRFLP peaks represented between 5.2 and 25.3% of the total peak area for each sample (Fig. 6). Abundance profiles for this class suggest similar distribution patterns for the two bay samples with more *Alphaproteobacteria* detected in the gulf sediments (Fig. 6). Supporting this range and abundance, TRFLP peaks matching in silico TRF sizes for phylotypes 3G02-39 and LC1-35, clustering within the family *Hyphomicrobiaceae*, were detected at almost every depth, site, and time point and had the largest percentage of total peak area for any sequence (see Fig. S2 in the supplemental material). Additional *Alphaproteobacteria* lineages were more depth specific (e.g., *Rhodobacterales*-related phylotype LC1-30 was detected in the shallow depths of all four samples) and site specific (e.g., *Rhizobiales*-related LC1-25 was observed almost exclusively in bay sediments profiles with relatively high peak areas [see Fig. S2 in the supplemental material]).

Classwide comparisons for both *Gamma-* and *Deltaproteobacteria* indicated larger peak areas below 8 cm in bay sediments and below 14 cm in gulf sediments (Fig. 6). For example, all three *Deltaproteobacteria*-related phylotypes were observed only in the deeper sediment depths. With the exception of phylotype 3B1820-38, bay *Deltaproteobacteria*-related phylotypes were detected higher in the sediment column, i.e., between 4 and 8 cm, compared to the gulf phylotypes (see Fig. S2 in the supplemental material). *Deltaproteobacteria*-related phylotypes were also detected higher in the column in May compared to March at both sites.

Multiple non-*Proteobacteria*-related phylotypes were detected and showed similar site, depth, and time specificity. *Pirellula*-related phylotypes were detected at mid-depths in bay and gulf samples (Fig. 6), whereas *Actinobacteria*-related phylotypes from bay sediments were observed higher in the sediment column compared to those detected in gulf sediments (Fig. 6). *Firmicutes*-related phylotypes 3G02-02 and 3B1820-01 clustered with the families *Paenibacillaceae* and *Turicibacteraceae*, respectively (see Table S2 in the supplemental material and Fig. 2) and were only detected in the shallow sediment depth TRFLP profiles (Fig. 6).

Similar to the community fingerprints of the SSU rRNA gene, approximately half of the TRFLP peaks from the *nosZ* fingerprints were identified and given a corresponding phylotype. Although numerous phylotypes were detected in both the bay and gulf samples including several that were detected at nearly all depths (i.e., SC3N-21/SC1N-18, SC3N-27, SC3N-19; see Fig. S3 in the supplemental material), some phylotypes were exclusive to one site or detected at limited depths within the cores. Peaks associated with phylotypes 3G1820N-06, 3G1820N-48, and SC3N-10 were detected on both sample dates but only in gulf sediments (see Fig. S3 in the supplemental material). A total of 87% of the clones detected in phylotype 3G02N-02 were isolated from gulf samples and 78% of these were in 3G02N (see Table S4 in the supplemental material). This is in agreement with TRFLP peak areas associated with this phylotype being much higher, with wider distribution through the gulf samples (see Fig. S3 in the supplemental material). More than 30% of the TRFLP peak area in the shallow bay sediment samples was associated with the phylotype 3G1820N-14 (10% of the total *nosZ* clones). Interestingly, this phylotype was not detected at any depth or time point in gulf sediments.

DISCUSSION

Our results from the NEGOM demonstrate that the diversity, as well as the metabolic activity, of bacterial communities is high in permeable sediment environments, likely due to increased transport of growth substrates and the removal of metabolites by advective exchange with the overlying water column (20). Using our expanded sequence database, the present study elucidated an unprecedented diversity of overall and denitrifying bacterial communities in marine sands (33, 55), and we expanded current knowledge to show the presence of numerous taxa that had not been previously recognized in marine sands. We further suggest that the *Gammaproteobacteria* are poised to respond rapidly to the input of growth substrates based on their relative abundance in rRNA clone libraries, although this observation should be tested by using more quantitative methods.

Phylogenetic analysis of the total and metabolically active bacterial communities in marine sands. Similar to previous studies of marine sediments (12, 33, 44, 45, 55), as well as of marine bacterioplanktonic communities (72), we showed that the *Gammaproteobacteria*, *Planctomycetes*, and *Bacteroidetes* groups predominate over the sequence diversity of marine sands. In contrast to previous work (45, 55), we observed that

FIG. 2. Non-*Proteobacteria* neighbor-joining phylogenetic tree, incorporating a Jukes-Cantor distance correction, of SSU rRNA gene sequences from 3B02, 3B1820, 3G02, and 3G1820 samples. Sequences from the present study and close relatives were aligned by using the Fast Aligner algorithm, verified by hand, and compared to the *E. coli* SSU rRNA secondary structure using the ARB software package. Sequence names in boldface type represent both cloned sequences and sequences from Hunter et al. (33) used in TRFLP peak analysis. Bootstrap analyses were conducted on 1,000 samples, and percentages greater than 50% are indicated at the nodes. *Methanococcus maripaludid* was used as the outgroup. Scale bar, 0.10 change per nucleotide position. Abbreviations: *Plancto*.(F), *Planctomycetaceae*; *Plancto*.(O), *Planctomycetales*; *Chrooc*., *Chroocales*; *Chlorob*.(F), *Chlorobiaceae*; *Chlorob*.(O), *Chlorobiales*; *Sphingo*., *Sphingobacteriales*; *Flavo*.(F), *Flavobacteriaceae*; *Flavo*.(O); *Flavobacteriales*; *Gemma*.(F), *Gemmatimonadaceae*; *Gemma*.(O), *Gemmatimonadales*; *Acido*.(F), *Acidobacteriaceae*, *Acido*.(O), *Acidobacteriales*; *Paeni*., *Paenibacillaceae*; *Turici*., *Turicibacteraceae*; *Anaero*.(F), *Anaerolinaceae*; *Anaero*.(O), *Anaerolinales*.

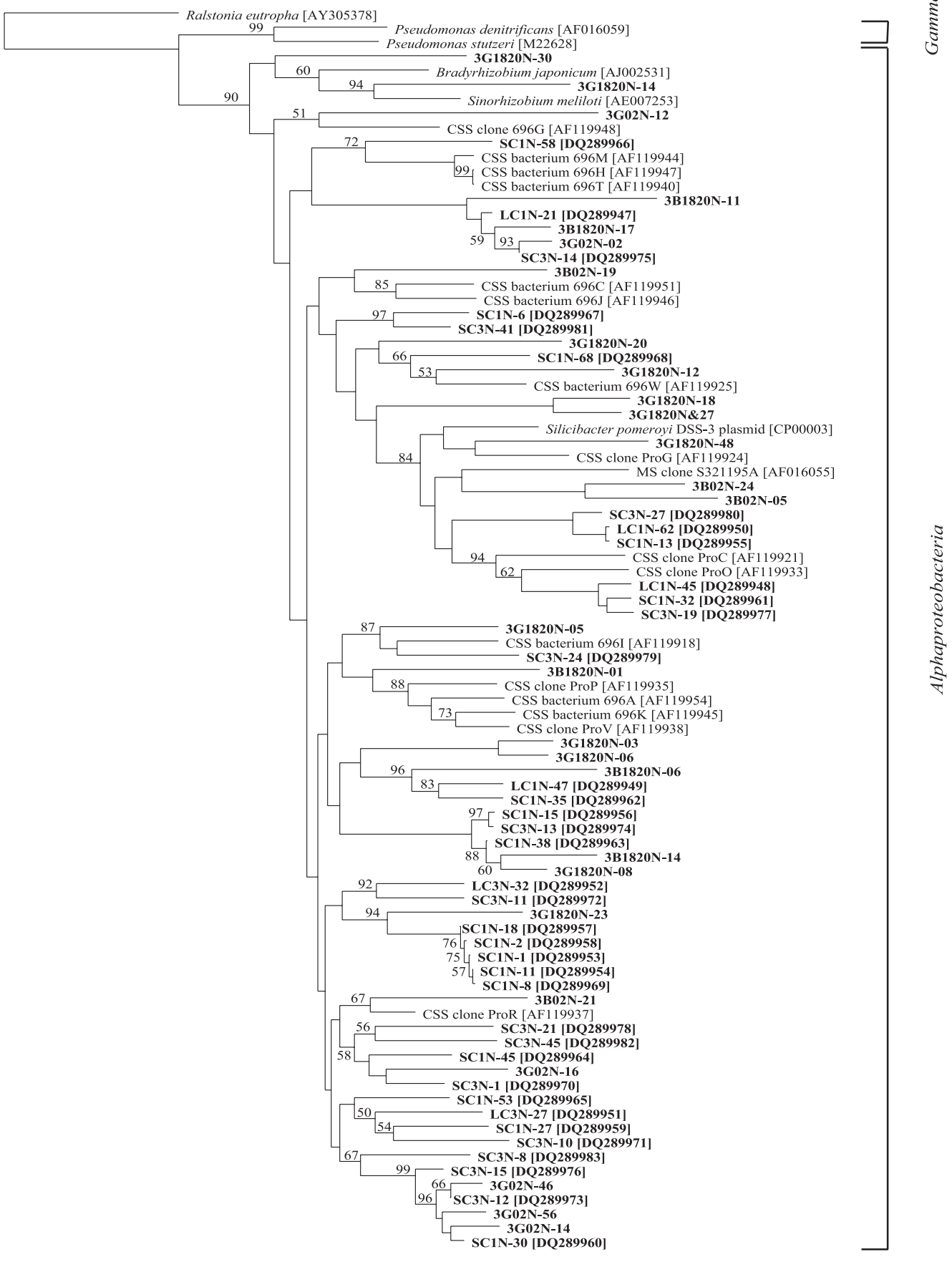
Ralstonia eutropha [AY305378]
Pseudomonas denitrificans [AF016059]
Pseudomonas stutzeri [M22628]
3G1820N-30
Bradyrhizobium japonicum [AJ002531]
3G1820N-14
Sinorhizobium meliloti [AE007253]
3G02N-12
CSS clone 696G [AF119948]
SC1N-58 [DQ289966]
CSS bacterium 696M [AF119944]
CSS bacterium 696H [AF119947]
CSS bacterium 696T [AF119940]
3B1820N-11
LC1N-21 [DQ289947]
3B1820N-17
3G02N-02
SC3N-14 [DQ289975]
3B02N-19
CSS bacterium 696C [AF119951]
CSS bacterium 696J [AF119946]
SC1N-6 [DQ289967]
SC3N-41 [DQ289981]
3G1820N-20
SC1N-68 [DQ289968]
3G1820N-12
CSS bacterium 696W [AF119925]
3G1820N-18
3G1820N&27
Silicibacter pomeroyi DSS-3 plasmid [CP00003]
3G1820N-48
CSS clone ProG [AF119924]
MS clone S321195A [AF016055]
3B02N-24
3B02N-05
SC3N-27 [DQ289980]
LC1N-62 [DQ289950]
SC1N-13 [DQ289955]
CSS clone ProC [AF119921]
CSS clone ProO [AF119933]
LC1N-45 [DQ289948]
SC1N-32 [DQ289961]
SC3N-19 [DQ289977]
3G1820N-05
CSS bacterium 696I [AF119918]
SC3N-24 [DQ289979]
3B1820N-01
CSS clone ProP [AF119935]
CSS bacterium 696A [AF119954]
CSS bacterium 696K [AF119945]
CSS clone ProV [AF119938]
3G1820N-03
3G1820N-06
3B1820N-06
LC1N-47 [DQ289949]
SC1N-35 [DQ289962]
SC1N-15 [DQ289956]
SC3N-13 [DQ289974]
SC1N-38 [DQ289963]
3B1820N-14
3G1820N-08
LC3N-32 [DQ289952]
SC3N-11 [DQ289972]
3G1820N-23
SC1N-18 [DQ289957]
SC1N-2 [DQ289958]
SC1N-1 [DQ289953]
SC1N-11 [DQ289954]
SC1N-8 [DQ289969]
3B02N-21
CSS clone ProR [AF119937]
SC3N-21 [DQ289978]
SC3N-45 [DQ289982]
SC1N-45 [DQ289964]
3G02N-16
SC3N-1 [DQ289970]
SC1N-53 [DQ289965]
LC3N-27 [DQ289951]
SC1N-27 [DQ289959]
SC3N-10 [DQ289971]
SC3N-8 [DQ289983]
SC3N-15 [DQ289976]
3G02N-46
SC3N-12 [DQ289973]
3G02N-56
3G02N-14
SC1N-30 [DQ289960]
Gamma.
Alphaproteobacteria
0.10

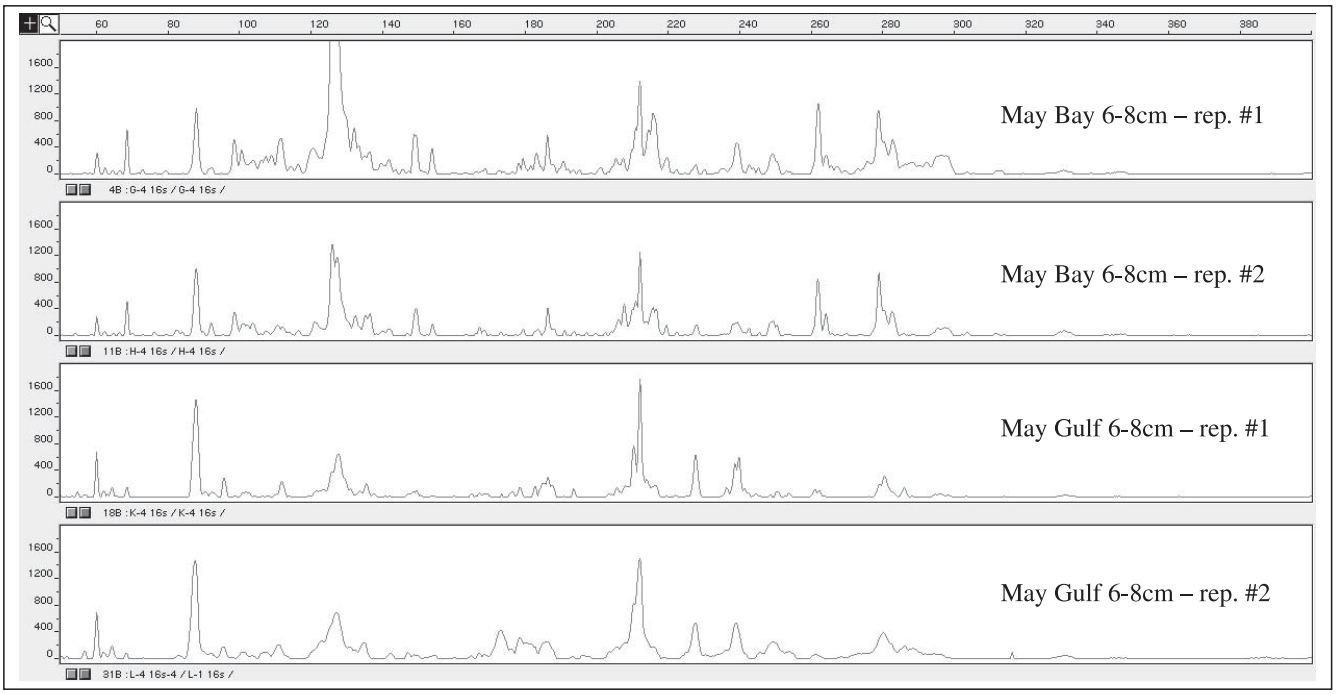

FIG. 4. Replicate TRFLP fingerprints of May bay and gulf 6- to 8-cm samples. Replicates from this depth demonstrate the reproducibility of TRFLP profiles from different cores collected at the same time and from the same site. Difference in peak presence and height can be observed between sites.

the *Alphaproteobacteria* showed the highest relative abundance in overall and denitrifying communities. The *Deltaproteobacteria* and gram-positive groups (*Actinobacteria* and *Firmicutes*) also comprised a substantial fraction of the overall diversity observed in permeable sediments, in agreement with previous work (12, 33, 45, 55). The relative abundance of *Alphaproteobacteria* phylotypes in particular suggests that this group is well adapted to sediments undergoing continuous and rapid pore water advection as indicated by the high permeability and rapid rates of organic matter turnover that we observed in the sands of the NEGOM. The fact that a predominance of *Alphaproteobacteria* sequences is also observed in marine bacterioplankton communities (72) may be explained by the recent observations showing enhanced exchange of particles between permeable sediments and the overlying water column (5, 18, 31, 36). In comparison to muddy marine sediments, bacteria could more readily switch between attached and planktonic lifestyles in marine sands.

A surprising observation of our study was that *Gammaproteobacteria*-related phylotypes were more frequently detected in RNA-derived clone libraries, suggesting high levels of metabolic activity within this group. Alternatively, *Gammaproteobacteria* found in the present study may maintain a higher ribosome content per cell under nongrowth conditions, as has been demonstrated in some pure cultures (22) and seawater enrichments (21). Regardless of the cause, increased rRNA levels may permit certain *Gammaproteobacteria* to respond better to the rapid changes in oxygen and organic substrates that occur in marine sands. One genus with the capacity for denitrification, i.e., *Marinobacter* (64), was detected within both gulf and bay sediment RNA-derived libraries, and previous cultivation work suggests that this group is among the most abundant of denitrifiers in marine sediments (4, 25). Specifically targeting this lineage with quantitative PCR methods would provide valuable insight into its ecological impact.

The results from the denitrifying communities are consistent with the rRNA findings with a large sequence diversity detected. However, *nosZ*-based phylogenetic classification beyond the class level, i.e., *Alphaproteobacteria*, is tentative at best. Linking *nosZ* diversity with SSU rRNA diversity is difficult due to primarily partial *nosZ* sequences from environmental samples being predominant in the database. Although additional marine denitrifiers have been cultured (62), gaps exist in the sequence database between SSU rRNA and *nosZ* phylogenies. For example, while *Hyphomicrobiaceae*, a family with known denitrifying lineages, was frequently detected in the DNA libraries, no *nosZ* genes and no full genome sequences for this group are available in public databases. Thus, many

FIG. 3. Neighbor-joining phylogenetic tree, incorporating a Jukes-Cantor distance correction, of the *nosZ* gene sequences from 3B02, 3B1820, 3G02, and 3G1820 samples. Sequences from the present study and close relatives were aligned by using the Fast Aligner algorithm and verified by hand by using the ARB software package. Sequence names in boldface type represent both cloned sequences and sequences from Hunter et al. (33) used in TRFLP peak analysis. Bootstrap analyses were conducted on 1,000 samples, and percentages greater than 50% are indicated at the nodes. *Ralstonia eutropha* strain H16 was used as the outgroup. Scale bar, 0.10 change per nucleotide position.

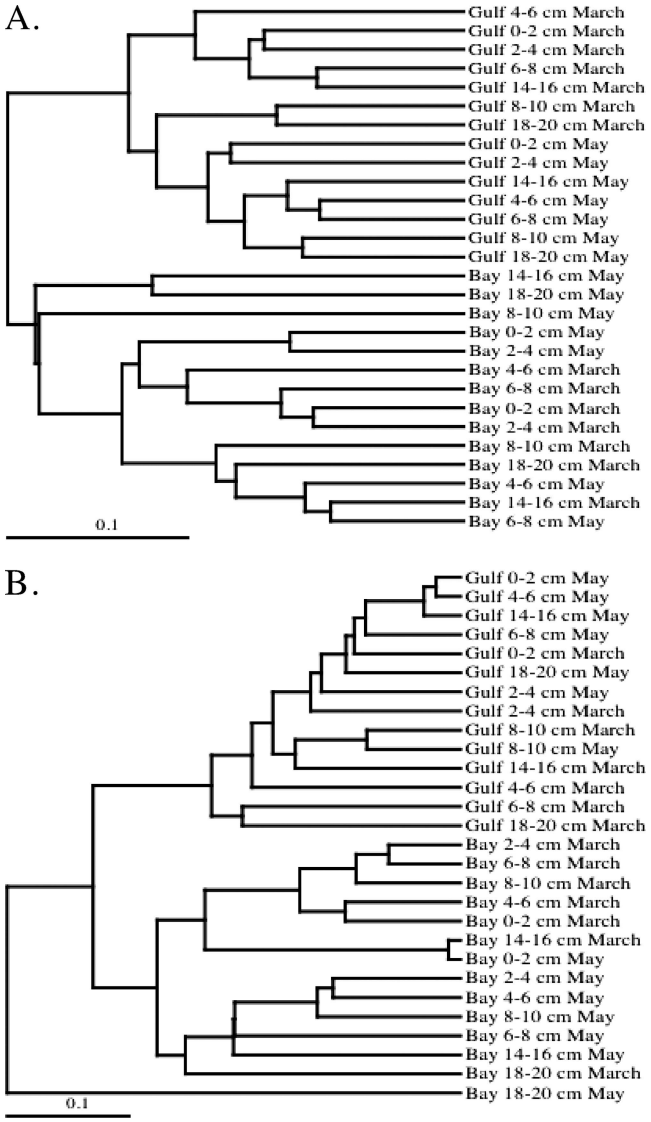

FIG. 5. Sorensen's index-based dendrograms of SSU rRNA gene (A) and *nosZ* gene (B). TRFLP profiles from each depth, site, and time were compared for peak absence or presence to produce a distance matrix pairwise comparison. Neighbor-joining trees were then constructed from the distance matrices.

nosZ sequences from the present study remain tightly clustered with previously reported clone sequences from environmental samples (33, 66) and not to cultivated species. These results underscore the need for cultivation of marine denitrifying model microorganisms that better represent the indigenous populations.

Analysis of the *amoA* gene showed a low diversity ($n = 2$) in NEGOM sediments in comparison with previous studies of marine muds (3, 13, 23, 58, 60). Bacterial *amoA* sequences showed a high sequence identity (98%) to sequences retrieved from the water column and muddy sediments of other coastal marine ecosystems. However, two ubiquitous phylotypes at both NEGOM sites represent a comparable level of diversity to a previous sandy sediment study (33). Therefore, while ammonia oxidation has been shown to play a critical role in the coastal ecosystem in other marine habitats (1, 8, 29, 49, 51, 57, 73), results presented here suggest that ammonia oxidizing-related taxa may be under-represented in these clone libraries, potentially due to targeting only the bacterial contribution to the ammonia oxidizing community (22a).

Profiling of permeable marine sediment communities over expanded scales using DNA fingerprinting. An understanding of bacterial community structure and function in marine sediments has been hampered by the excessive time and cost of sample processing. Previous studies of bacterial diversity in marine sediments have relied mainly on clonal analysis and have often lacked replication or based interpretation of bacterial community structure on relatively few samples. In the present study, DNA fingerprinting provided improved replication and spatial coverage that was not achievable with clonal analysis. Consistent with past work in marine sands (55), we observed community composition at the phylum/subphylum level to be relatively stable in clone libraries, whereas we observed substantial trends with depth and between sites at the

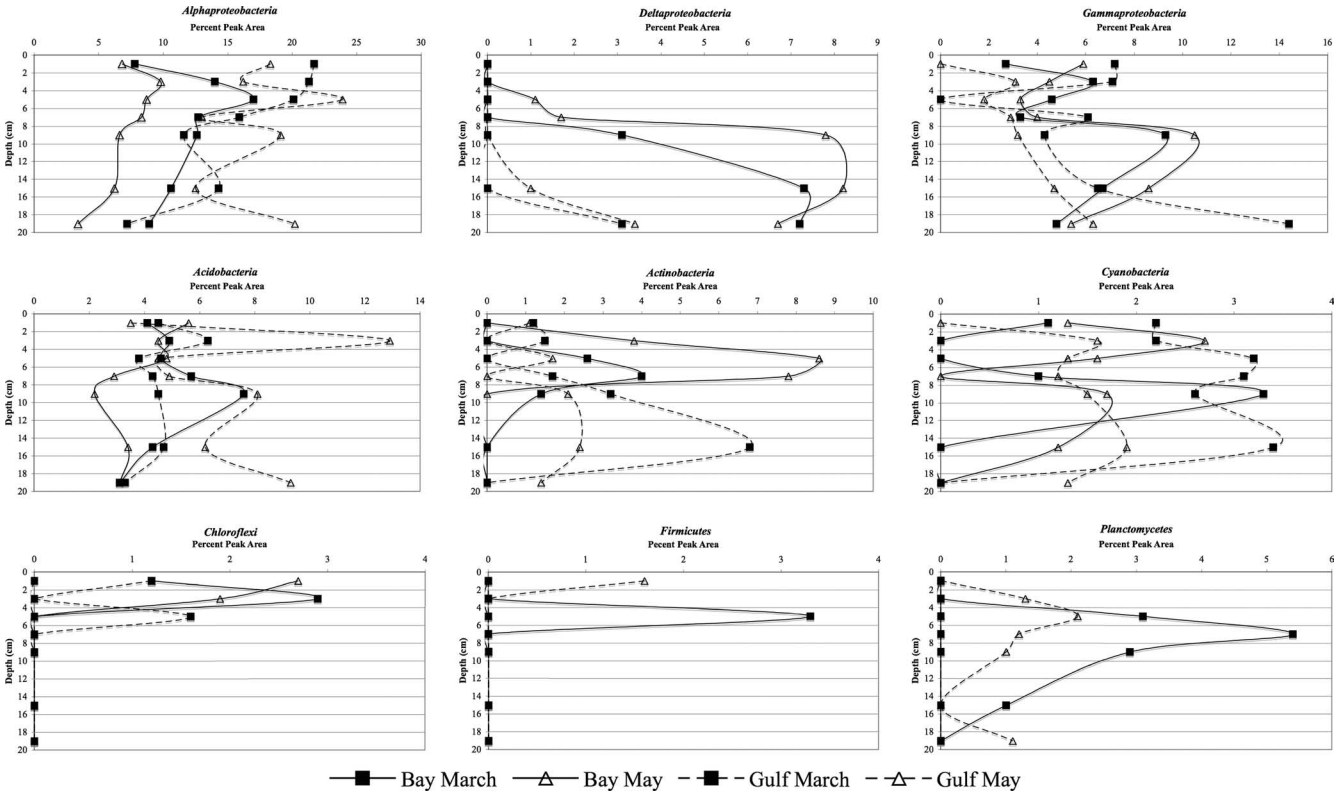

FIG. 6. Relative abundance of microbial populations across sediment depth, site and time. Phylogenetic groups were determined by comparing in silico digests of cloned sequences to electropherogram peak sizes during TRFLP analysis. The percentage of the total peak area was then reported for each clone and combined with similar lineages to produce abundance profiles. TRFLP peak area profiles for *Gemmatimonadetes* were omitted due to a single clone detected in March Gulf samples from 4 to 10 cm. Please note the differences in *x*-axis scales.

family to species level using our community fingerprinting approach. Such differences in community interpretation highlight the need for more robust replication in sampling and characterization. The results presented here are indicative of in situ conditions, not total community potential as shown by the microcosm experiments of Hunter et al. (33).

Sorensen's index-based analysis of TRFLP profiles provided evidence for bacterial niche specialization and suggested that the bacterial community diversity is affected by advective pore water flow in permeable sands. The gulf site was exposed to higher flushing rates due to increased exposure to larger waves compared to bay site sediments. Lower sediment flushing rates and a well-defined redox gradient, as determined by a clearly visible zone of black iron sulfides at a depth of ~4 cm, were observed in the bay sediments. These differences may thus lead to at least some of the variations in the community structure that were observed. By correlating specific TRFLP peaks to cloned sequences, changes in community structure at each depth interval could be analyzed for potential ecological impacts. Two *Alphaproteobacteria* phylotypes were related to a known denitrifier, i.e., *Hyphomicrobium denitrificans* strain DSM 1869 (62), and were detected at all sites, depths, and time points, thus supporting the broad distribution observed in a previous lab-based sandy sediment community structure determination (33). *Hyphomicrobiaceae* lineages have been detected in a wide variety of environments (i.e., wastewater [19], deep-sea sediment [53, 74], and Antarctic sediment 52]) and linked not only to nitrogen cycling but also to growth on methylated sulfur compounds (52). Such metabolically diverse lineages with the capacity for denitrification may prove to be a significant contributor to geochemical processes in dynamic environments such as coastal sediments that are subjected to variable pulses of carbon and oxygen. At deeper depths, *Deltaproteobacteria* (i.e., *Desulfobulbaceae* and *Desulfobacteraceae*) became more relatively abundant, supporting the location of the redox boundary as observed by the presence of iron sulfides in the cores. Due to pore water flow within these sediments, it is interesting to hypothesize that the depth-specific taxa identified are surface adherent and thus less affected by water influx.

Large differences in community structure with depth were expected, and the differences in the distribution of bacterial taxa between sites at comparable depth are consistent with prior findings in coastal sands from the Mid-Atlantic Bight (67). The Sorensen's index-based analysis of the TRFLP profiles indicated as low as 50% similarity for SSU rRNA gene and 38% similarity for *nosZ* between the bay and gulf bacterial communities. Thus, differences in flushing rates or redox zone stability may allow different populations to become more numerous between sites. Free-living, non-surface-adherent populations (26) may be forced by pore water flow through the sediment and thus detected at multiple locations within the core. Such movement within the sediment may explain why some groups (i.e., denitrifiers and phototrophs) were detected throughout the core despite having limited geochemical ranges.

Vertical and lateral movement of sediment particles may also contribute to site-specific similarities in the bacterial community structure. Although wave action and bottom water currents can suspend and mix surface sediments (61, 65), homogenization may be limited to only the uppermost sediment layers. Surface-adherent populations would then be less mixed throughout the core compared to the effect of advective flow on free-living populations. Such mixing would explain the broad depth range of some detected lineages within the present study, including the aforementioned *Deltaproteobacteria* taxa. In addition, members of the *Rhodobacteraceae* and *Cyanobacteria* are known phototrophs; however, their profiles within the sediment were very different. While *Rhodobacteraceae* were detected in the shallow depths exclusively, *Cyanobacteria*-related lineages were observed at all depths.

ACKNOWLEDGMENTS

This study was supported by grants from the National Science Foundation (OCE-0424967 and OCE-0726754) and Florida State University (PEG 513680014). J.E.K. was supported in part by a fellowship from the Hanse Wissenschaftskolleg during the preparation of the manuscript. We also acknowledge the logistical support of the FSU Coastal and Marine Laboratory.

REFERENCES

1. **Asami, H., M. Aida, and K. Watanabe.** 2005. Accelerated sulfur cycle in coastal marine sediment beneath areas of intensive shellfish aquaculture. Appl. Environ. Microbiol. **71:**2925–2933.
2. **Barnett, M. J., R. F. Fisher, T. Jones, C. Komp, A. P. Abola, F. Barly-Hubler, L. Bowser, D. Capela, F. Galibert, J. Gouzy, M. Gurjal, M. Hong, L. Huizar, R. W. Hyman, D. Kahn, M. L. Kahn, S. Kalman, D. H. Keating, C. Palm, M. C. Peck, R. Surzycki, D. H. Wells, K. Yeh, R. W. Davis, N. A. Federspiel, and S. R. Long.** 2001. Nucleotide sequence and predicted functions of the entire *Sinorhizobium meliloti* pSymA megaplasmid. Proc. Natl. Acad. Sci. USA **98:**9883–9888.
3. **Bernhard, A. E., T. Donn, A. E. Giblin, and D. A. Stahl.** 2005. Loss of diversity of ammonia-oxidizing bacteria correlates with increasing salinity in an estuary system. Environ. Microbiol. **7:**1289–1297.
4. **Bhatt, M., J. S. Zhao, F. Monteil-Rivera, and M. Hawari.** 2005. Biodegradation of cyclic nitramines by tropical marine sediment bacteria. J. Indust. Microbiol. Biotechnol. **32:**261–267.
5. **Billerbeck, M., U. Werner, L. Polerecky, E. Walpersdorf, D. de Beer, and M. Huettel.** 2006. Surficial and deep pore water circulation governs spatial and temporal scales of nutrient recycling in intertidal sand flat sediment. Mar. Ecol. Prog. Ser. **326:**61–76.
6. **Blott, S. J., and K. Pye.** 2001. Gradistat: a grain size distribution and statistics package for the analysis of unconsolidated sediments. Earth Surf. Proc. Landf. **26:**1237–1248.
7. **Boudreau, B. P., M. Huettel, S. Forster, R. A. Jahnke, A. McLachlan, J. J. Middelburg, P. Nielsen, F. Sansone, G. Taghon, W. Van Raaphorst, et al.** 2001. Permeable marine sediments: overturning an old paradigm. EOS Trans. AGU **82:**133–140.
8. **Bowman, J. P., and R. D. McCuaig.** 2003. Biodiversity, community structural shifts, and biogeography of prokaryotes within Antarctic continental shelf sediment. Appl. Environ. Microbiol. **69:**2463–2483.
9. **Braker, G., H. L. Ayala-del-Rio, A. H. Devol, A. Fesefeldt, and J. M. Tiedje.** 2001. Community structure of denitrifiers, *Bacteria*, and *Archaea* along redox gradients in Pacific Northwest marine sediments by terminal restriction fragment length polymorphism analysis of amplified nitrite reductase (*nirS*) and 16S rRNA genes. Appl. Environ. Microbiol. **67:**1893–1901.
10. **Braker, G., J. Z. Zhou, L. Y. Wu, A. H. Devol, and J. M. Tiedje.** 2000. Nitrite reductase genes (*nirK* and *nirS*) as functional markers to investigate diversity of denitrifying bacteria in Pacific Northwest marine sediment communities. Appl. Environ. Microbiol. **66:**2096–2104.
11. **Buhring, S. I., S. Ehrenhauss, A. Kamp, L. Moodley, and U. Witte.** 2006. Enhanced benthic activity in sandy sublittoral sediments: evidence from 13C tracer experiments. Mar. Biol. Res. **2:**120–129.
12. **Buhring, S. I., M. Elvert, and U. Witte.** 2005. The microbial community structure of different permeable sandy sediments characterized by the investigation of bacterial fatty acids and fluorescence in situ hybridization. Environ. Microbiol. **7:**281–293.
13. **Caffrey, J. M., N. Harrington, I. Solem, and B. B. Ward.** 2003. Biogeochemical processes in a small California estuary: nitrification activity, community structure, and role in nitrogen budgets. MEPS **248:**27–40.
14. **Chao, A.** 1987. Estimating the population size for capture-recapture data with unequal catchability. Biometrics **43:**783–791.
15. **Christensen, J. P.** 1994. Carbon export from continental shelves, denitrification and atmospheric carbon-dioxide. Cont. Shelf Res. **14:**547–576.
16. **Colwell, R. K.** 1997. EstimateS: statistical estimation of species richness and shared species from samples, version 5. User's guide and application. http://viceroy.eeb.uconn.edu/estimates.
17. **Colwell, R. K., and J. A. Coddington.** 1994. Estimating terrestrial biodiversity through extrapolation. Philos. Trans. R. Soc. Lond. B **345:**101–118.
18. **Cook, P. L. M., F. Wenzhofer, R. N. Glud, F. Janssen, and M. Huettel.** 2007. Benthic solute exchange and carbon mineralization in two shallow subtidal sandy sediments: effect of advective pore-water exchange. Limnol. Oceanogr. **52:**1943–1963.
19. **Costa, C., C. Dijkema, M. Friedrich, P. Garcia-Encina, F. Fernandez-Polanco, and A. J. M. Stams.** 2000. Denitrification with methane as electron donor in oxygen-limited bioreactors. Appl. Microbiol. Biotechnol. **53:**754–762.
20. **Ehrenhauss, S., U. Witte, S. L. Buhring, and M. Huettel.** 2004. Effect of advective pore water transport on distribution and degradation of diatoms in permeable North Sea sediments. Mar. Ecol. Prog. Ser. **271:**99–111.
21. **Eilers, H., J. Pernthaler, and R. Amann.** 2000. Succession of pelagic marine bacteria during enrichment: a close look at cultivation-induced shifts. Appl. Environ. Microbiol. **66:**4634–4649.
22. **Flaerdh, K., P. S. Cohen, and S. Kjelleberg.** 1992. Ribosomes exist in large excess over the apparent demand for protein synthesis during carbon starvation in marine *Vibrio* sp. strain CCUB 15956. J. Bacteriol. **174:**6780–6788.

22a. **Francis, C. A., K. J. Roberts, J. M. Beman, A. E. Santoro, and B. B. Oakley.** 2005. Ubiquity and diversity of ammonia-oxidizing archaea in water columns and sediments of the ocean. Proc. NaH. Acad. Sci. USA **102:**14683–14688.

23. **Francis, C. A., G. D. O'Mullan, and B. B. Ward.** 2003. Diversity of ammonia monooxygenase (*amoA*) genes across environmental gradients in Chesapeake Bay sediments. Geobiology **1:**129–140.

23a. **Giovannoni, S. J.** 1991. The polymerase chain reaction, p. 177–203. *In* E. Stackebrandt and M. Goodfellow (ed.), Nucleic acid techniques in bacterial systematics. Wiley, Chichester, United Kingdom.

24. **Good, I. J.** 1953. The population frequencies of species and the estimation of population parameters. Biometrika **40:**237–264.
25. **Goregues, C. M., V. D. Michotey, and P. C. Bonin.** 2005. Molecular, biochemical, and physiological approaches for understanding the ecology of denitrification. Microb. Ecol. **49:**198–208.
26. **Harvey, R. W., L. H. George, R. L. Smith, and D. R. Leblanc.** 1989. Transport of microspheres and indigenous bacteria through a sandy aquifer: results of natural-gradient and forced-gradient tracer experiments. Environ. Sci. Technol. **23:**51–56.
27. **Heck, K. L., G. V. Belle, and D. Siberloff.** 1975. Explicit calculation of the rarefaction diversity measurement and the determination of sufficient sample size. Ecology **56:**1459–1461.
28. **Holme, N. A., and A. D. McIntyre.** 1984. Methods for the study of marine benthos. Blackwell Scientific Publications, London, England.
29. **Holmes, A. J., N. A. Tujula, M. Holley, A. Contos, J. M. James, P. Rogers, and M. R. Gillings.** 2001. Phylogenetic structure of unusual aquatic microbial formations in Nullarbor caves, Australia. Environ. Microbiol. **3:**256–264.
30. **Howarth, R. W., and R. Marino.** 2006. Nitrogen as the limiting nutrient for eutrophication in coastal marine ecosystems: evolving views over three decades. Limnol. Oceanogr. **51:**364–376.
31. **Huettel, M., P. L. M. Cook, F. Janssen, G. Lavik, and J. J. Middelburg.** 2007. Transport and degradation of a dinoflagellate bloom in permeable sublittoral sediment. Mar. Ecol. Prog. Ser. **340:**139–153.
32. **Huettel, M., W. Ziebis, and S. Forster.** 1996. Flow-induced uptake of particulate matter in permeable sediments. Limnol. Oceanogr. **41:**309–322.
33. **Hunter, E. M., H. J. Mills, and J. E. Kostka.** 2006. Microbial community diversity associated with carbon and nitrogen cycling in permeable marine sediments. Appl. Environ. Microbiol. **72:**5689–5701.
34. **Jahnke, R., M. Richards, J. Nelson, C. Robertson, A. Rao, and D. Jahnke.** 2005. Organic matter remineralization and porewater exchange rates in permeable South Atlantic Bight continental shelf sediments. Cont. Shelf Res. **25:**1433–1452.
35. **Jahnke, R. A., J. R. Nelson, R. L. Marinelli, and J. E. Eckman.** 2000. Benthic flux of biogenic elements on the Southeastern US continental shelf: influence of pore water advective transport and benthic microalgae. Cont. Shelf Res. **20:**109–127.
36. **Janssen, F., M. Huettel, and U. Witte.** 2005. Pore-water advection and solute fluxes in permeable marine sediments (II): benthic respiration at three sandy sites with different permeabilities (German Bight, North Sea). Limnol. Oceanogr. **50:**779–792.
37. **Joergensen, B. B.** 2000. Bacteria and marine biogeochemistry, p. 173–207. *In* H. D. Schultz and M. Zabel (ed.), Marine geochemistry. Springer-Verlag, Berlin, Germany.
38. **Joergensen, B. B.** 1996. Material flux in the sediment, p. 115–135. *In* B. B. Jorgensen and K. Richardson (ed.), Eutrophication in coastal marine ecosystems. ASLO, Waco, TX.
39. **Johnson, J. A., V. Ravi, and J. K. Rumery.** 1994. Estimation of solute

concentrations using the pathline counting method. Ground Water **32:**719–726.

40. **Kerkhof, L., and M. Speck.** 1997. Ribosomal RNA gene dosage in marine bacteria. Mol. Mar. Biol. Biotechnol. **6:**260–267.
41. **Kerkhof, L. J., and B. B. Ward.** 1993. Comparison of nucleic acid hybridization and fluorometry for measurement of RNA/DNA relationship with growth rate in a marine bacterium. Appl. Environ. Microbiol. **59:**1303–1307.

41a. **Lane, D. J., B. Pace, G. J. Olsen, D. A. Stahl, M. L. Sogin, and N. R. Pace.** 1985. Rapid determination of 16S ribosomal RNA sequences for phylogenetic analyses. Proc. Natl. Acad. Sci. USA **82:**6955–6959.

42. **Laursen, A. E., and S. P. Seitzinger.** 2002. The role of denitrification in nitrogen removal and carbon mineralization in Mid-Atlantic Bight sediments. Cont. Shelf Res. **22:**1397–1416.
43. **Liu, X. D., S. M. Tiquia, G. Holguin, L. Y. Wu, S. C. Nold, A. H. Devol, K. Luo, A. V. Palumbo, J. M. Tiedje, and J. H. Zhou.** 2003. Molecular diversity of denitrifying genes in continental margin sediments within the oxygen-deficient zone off the Pacific coast of Mexico. Appl. Environ. Microbiol. **69:**3549–3560.
44. **Llobet-Brossa, E., R. Rabus, M. E. Bottcher, M. Konneke, N. Finke, A. Schramm, R. L. Meyer, S. Grotzschel, R. Rossello-Mora, and R. Amann.** 2002. Community structure and activity of sulfate-reducing bacteria in an intertidal surface sediment: a multi-method approach. Aquat. Microb. Ecol. **29:**211–226.
45. **Llobet-Brossa, E., R. Rossello-Mora, and R. Amann.** 1998. Microbial community composition of Wadden Sea sediments as revealed by fluorescence in situ hybridization. Appl. Environ. Microbiol. **64:**2691–2696.
46. **Madigan, M. T., J. M. Martinko, and J. Parker.** 2006. Brock biology of microorganisms, 11th ed. Pearson Education, Inc., Upper Saddle River, NJ.
47. **Magurran, A. E.** 1988. Ecological diversity and its measurement. Princeton University Press, Princeton, NJ.
48. **Maidak, B. L., J. R. Cole, C. T. Parker, G. M. Garrity, N. Larsen, B. Li, T. G. Lilburn, M. J. McCaughey, G. J. Olsen, R. Overbeek, S. Pramanik, T. M. Schmidt, J. M. Tiedje, and C. R. Woese.** 1999. A new version of the RDP. Nucleic Acids Res. **27:**171–173.
49. **Matsui, G. Y., D. B. Ringelberg, and C. R. Lovell.** 2004. Sulfate-reducing bacteria in tubes constructed by the marine infaunal polychaete *Diopatra cuprea*. Appl. Environ. Microbiol. **70:**7053–7065.
50. **Messing, J.** 1983. New M13 vectors for cloning. Methods Enzymol. **101:**20–79.
51. **Mills, H. J., C. Hodges, K. Wilson, I. R. MacDonald, and P. A. Sobecky.** 2003. Microbial diversity in sediments associated with surface-breaching gas hydrate mounds in the Gulf of Mexico. FEMS Microbiol. Ecol. **46:**39–52.
52. **Moosvi, S. A., I. R. McDonald, D. A. Pearce, D. P. Kelly, and A. P. Wood.** 2005. Molecular detection and isolation from Antarctica of methylotrophic bacteria able to grow with methylated sulfur compounds. Syst. Appl. Microbiol. **28:**541–554.
53. **Mu, C. H., Z. M. Bao, G. Chen, J. J. Hu, L. J. Hao, Z. H. Qi, and G. X. Li.** 2005. Bacterial diversity in the sediments collected from the Shikoku Basin. Acta Oceanol. Sin. **24:**114–121.
54. **Mullins, T. D., T. B. Britschgi, R. I. Krest, and S. J. Giovannoni.** 1995. Genetic comparisons reveal the same unknown bacterial lineages in Atlantic and Pacific bacterioplankton communities. Limnol. Oceanogr. **39:**148–158.
55. **Musat, F., J. Harder, and F. Widdel.** 2006. Study of nitrogen fixation in microbial communities of oil-contaminated marine sediment microcosms. Environ. Microbiol. **8:**1834–1843.
56. **Musat, N., U. Werner, K. Knittel, S. Kolb, T. Dodenhof, J. E. E. van Beusekom, D. de Beer, N. Dubilier, and R. Amann.** 2006. Microbial community structure of sandy intertidal sediments in the North Sea, Sylt-Romo Basin, Wadden Sea. Syst. Appl. Microbiol. **29:**333–348.
57. **Mussmann, M., K. Ishii, R. Rabus, and R. Amann.** 2005. Diversity and vertical distribution of cultured and uncultured *Deltaproteobacteria* in an intertidal mud flat of the Wadden Sea. Environ. Microbiol. **7:**405–418.
58. **Nicolaisen, M. H., and N. B. Ramsing.** 2002. Denaturing gradient gel electrophoresis (DGGE) approaches to study the diversity of ammonia-oxidizing bacteria. J. Microbiol. Methods **50:**189–203.
59. **Nogales, B., E. R. B. Moore, W.-R. Abraham, and K. N. Timmis.** 1999. Identification of the metabolically active members of a bacterial community in a polychlorinated biphenyl-polluted moorland soil. Environ. Microbiol. **1:**199–212.
60. **Nold, S. C., J. Zhou, A. H. Devol, and J. M. Tiedje.** 2000. Pacific northwest marine sediments contain ammonia-oxidizing bacteria in the beta subdivision of the *Proteobacteria*. Appl. Environ. Microbiol. **66:**432–4535.
61. **Pilditch, C. A., and D. C. Miller.** 2006. Phytoplankton deposition to permeable sediments under oscillatory flow: effects of ripple geometry and resuspension. Cont. Shelf Res. **26:**1806–1825.
62. **Rainey, F. A., N. Ward-Rainey, C. G. Gliesche, and E. Stackebrandt.** 1998. Phylogenetic analysis and intrageneric structure of the genus *Hyphomicrobium* and the related genus *Filomicrobium*. Int. J. Syst. Bacteriol. **48:**635–639.
63. **Reimers, C. E., H. A. Stecher, G. L. Taghon, C. M. Fuller, M. Huettel, A. Rusch, N. Ryckelynck, and C. Wild.** 2004. In situ measurements of advective solute transport in permeable shelf sands. Cont. Shelf Res. **24:**183–201.
64. **Rontani, J. F., A. Mouzdahir, V. Michotey, and P. Bonin.** 2002. Aerobic and anaerobic metabolism of squalene by a denitrifying bacterium isolated from marine sediment. Arch. Microbiol. **178:**279–287.
65. **Rusch, A., and M. Huettel.** 2000. Advective particle transport into permeable sediments: evidence from experiments in an intertidal sandflat. Limnol. Oceanogr. **45:**525–533.
66. **Scala, D. J., and L. J. Kerkhof.** 1999. Diversity of nitrous oxide reductase (*nosZ*) genes in continental shelf sediments. Appl. Environ. Microbiol. **65:**1681–1687.
67. **Scala, D. J., and L. J. Kerkhof.** 2000. Horizontal heterogeneity of denitrifying bacterial communities in marine sediments by terminal restriction fragment length polymorphism analysis. Appl. Environ. Microbiol. **66:**1980–1986.
68. **Scala, D. J., and L. J. Kerkhof.** 1998. Nitrous oxide reductase (*nosZ*) gene-specific PCR primers for detection of denitrifiers and three *nosZ* genes from marine sediments. FEMS Microbiol. Lett. **162:**61–68.
69. **Schwinter, C., M. Sabaty, B. Berna, S. Cahors, and P. Richaud.** 1998. Plasmid content and localization of the genes encoding the denitrification enzymes in two strains of *Rhodobacter sphaeroides*. FEMS Microbiol. Lett. **165:**313–321.
70. **Seitzinger, S. P., and A. E. Giblin.** 1996. Estimating denitrification in North Atlantic continental shelf sediments. Biogeochemistry **35:**235–260.
71. **Strunk, O., and W. Ludwig.** 1997. ARB: software for phylogenetic analysis. Technishe Universitat München, Munich, Germany.
72. **Suzuki, M. T., O. Beja, L. T. Taylor, and E. F. DeLong.** 2001. Phylogenetic analysis of rRNA operons from uncultivated coastal marine bacterioplankton. Environ. Microbiol. **3:**323–331.
73. **Teske, A., K. U. Hinrichs, V. Edgcomb, A. D. Gomez, D. Kysela, S. P. Sylva, M. L. Sogin, and H. W. Jannasch.** 2002. Microbial diversity of hydrothermal sediments in the Guaymas Basin: evidence for anaerobic methanotrophic communities. Appl. Environ. Microbiol. **68:**1994–2007.
74. **Wang, P., F. P. Wang, M. X. Xu, and X. Xiao.** 2004. Molecular phylogeny of methylotrophs in a deep-sea sediment from a tropical west Pacific Warm Pool. FEMS Microbiol. Ecol. **47:**77–84.